THE JOURNAL OF THE ACOUSTICAL SOCIETY OF KOREA VOL.23, NO.2E 2004. 6 pp. 44-50

Sound Propagation over Multiple Wedges and Barriers

Hyun-Sil Kim* , Jae-Sueng Kim*, Hyun-Ju Kang*, Bong-Ki Kim*, Sang-Ryul Kim*
Acoustics Laboratory Korea Institute of Machinery and Materials
(Received February 16 2004; accepted August 30 2004)

Abstract

A theoretical formula that is based on the geometrical theory of diffraction (GTD) is proposed for computing sound diffraction by multiple wedges, barriers, and polygonal-like shapes. The formula can treat both convex and concave edges, where edges may or may not be inter-connected. Comparisons of theoretical predictions with other results done by the BEM or experiments for scaled model confirm the accuracy of the present formula. Numerical examples such as double wedges and doubly inclined barrier show that when there exist several diffraction paths for given source and receiver positions, the insertion loss is dominated by the diffraction associated with the shortest propagation path.

Keywords: *Multiple diffraction, Geometrical theory of diffraction, Barrier, Wedge*

Ⅰ. Introduction

Sound wave propagation over obstacles such as noise barriers and buildings are of great importance in many practical applications. The simplest problem is single diffraction of sound by a screen or wedge, for which numerous works have been done and an excellent literature review can be found in the paper by Ouis[1]. Among various theories on diffraction, the geometrical theory of diffraction (GTD[2-4]) has been widely used due to its relative easiness in numerical implementation and its accuracy is sufficient from the view point of engineering applications. Salomons[5] compared GTD with other methods such as BEM, parabolic equation method, and experimental results, and remarked that GTD is a fast and accurate tool for many practical applications for noise barriers. Originally, the GTD have been developed in electromagnetic waves, where high frequency diffraction is important in radar design .

Corresponding author: Hyun-Sil Kim (hskim@kimm.re.kr)
Acoustics Laboratory Korea Institute Machinery and Materials
305-343 Yu-Sung Gu, Jang-Dong 171, Taejon, Korea

When sound propagates over thick barrier or polygonal-like obstacle, there occur multiple diffractions. Pierce[3] derived formula for double diffractions over a thick barrier by extending his GTD given for single edge. Kawai[6] extended Pierce's idea to multiple diffraction by a many-sided barrier or pillar that consist of convex edges. Jin *et al.* [7] applied Kawai's expression to compute insertion loss of a partially inclined barrier, where they included diffractions occurred both at convex and concave edges. Robertson[8] and Ouis[1] also considered convex and concave edges in a wedge-like barrier on the ground.

Kawai's expression[6] based on GTD can be generalized to more complex configurations having an arbitrary number of convex and concave edges, provided that all edges are inter-connected by the common side plane. Salomons[5] proposed a method to deal with multiple arbitrarily placed barriers. However, his solution suffers from a numerical difficulty as discussed in Ref. [9].

For double barriers where two knife-edge barriers are separated, Wadsworth and Chambers[9] used the Biot-Tolstoy-Medwin's (BTM) method[10] in computing insertion loss. Although the BTM can handle general configurations in multiple diffraction and does not require

the edges to be connected, it is a time domain formulation, and needs FFT to obtain the frequency contents.

In this paper, we propose a method based on GTD to compute sound diffractions by multiple wedges, barriers, and polygonal-like shapes, where edges may or may not be inter-connected. We use the GTD developed by Kouyoumjian and Pathak[2], since it can handle concave edge and is more accurate compared to other GTDs as discussed in Refs. [1] and [6]. We investigate the accuracy of the present method by comparing the predictions to other results done by BEM or measurements. For numerical examples, we consider double and triple barriers, double wedges, and doubly inclined barriers. We also study the contributions from different diffraction paths when there exist several propagation paths.

II. Theoretical analysis

We consider a wedge in Fig. 1, where we use a cylindrical coordinate system (r,θ,z). The radial distance and angle of the source S, and receiver point R with respect to edge point Q are (R_S,θ_S), and (R_R,θ_R) respectively, whereas the edge angle is defined as $\nu\pi$. The diffracted wave field at receiver point R is given by [2]

$$\phi = \phi_i(Q) D_Q M e^{-ikR_R} \tag{1}$$

where $\phi_i(Q)$ is the incident wave at point Q, D_Q the diffraction coefficient, M the scale factor. In this paper, we assume the time dependence as $e^{i\omega t}$. For spherical wave incidence (we consider here only the normal incidence to

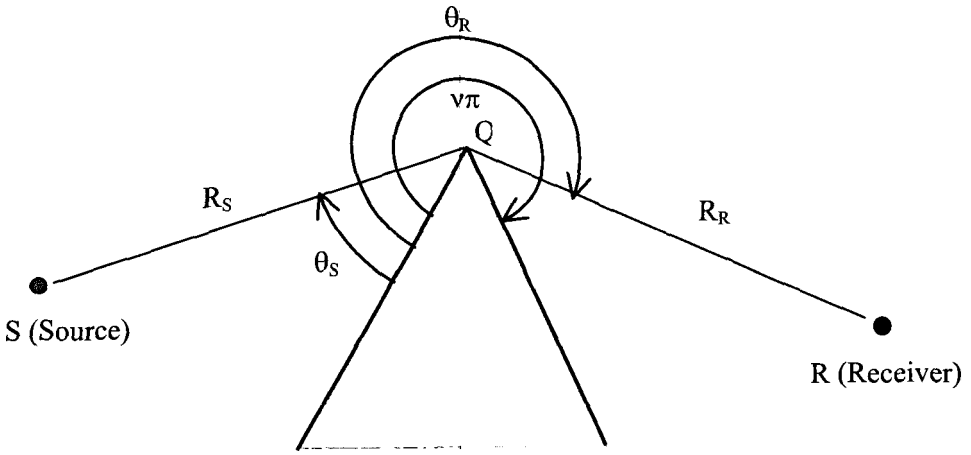

Fig. 1 Single diffraction by a wedge

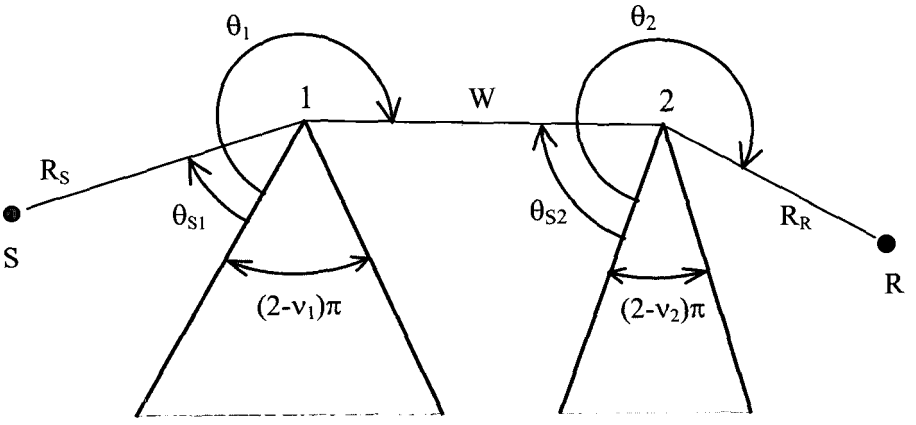

Figure 2. Double diffraction by two wedges

the edge. For oblique incidence, a minor change is needed. See Ref. [2] for details), we have

$$\phi_i(Q) = \frac{e^{-ikR_S}}{R_S},\ M = \sqrt{\frac{R_S}{R_R(R_S+R_R)}}, \tag{2}$$

while for cylindrical wave incidence, $M = 1/\sqrt{R_R}$, and $\phi_i(Q)$ is replaced by Hankel function, $(-i/4)H_0^{(2)}(kR_S)$.

The diffraction coefficient D_Q can be expressed as [2]

$$D_Q = V_Q(A,B,\theta_R - \theta_S) + V_Q(A,B,\theta_S + \theta_R), \tag{3}$$

in which $A = R_S R_R/(R_S + R_R)$ and

$$V_Q(A,B,\Theta) = -\frac{e^{-i\pi/4}}{\sqrt{2\pi k}}\frac{1}{2\nu}\cot\frac{\pi \pm \Theta}{2\nu}F^*\{BX_Q^{\pm}(\Theta)\}. \tag{4}$$

The coefficient B is introduced for multiple diffraction, where $B = 1$ for single diffraction.

The function $F^*(x)$, related to the Fresnel integral, is given by

$$F^*(x) = 2i\sqrt{x}\exp(ix)\int_{\sqrt{x}}^{\infty}\exp(-i\tau^2)d\tau, \tag{5}$$

and

$$X_Q^{\pm}(\theta) = 2kA\cos^2\left(\frac{2N^{\pm}\nu\pi - \theta}{2}\right), \tag{6}$$

$$N^{+} = \begin{cases} 0 & \text{for } \theta \le \nu\pi - \pi \\ 1 & \text{for } \theta > \nu\pi - \pi \end{cases},\quad N^{-} = \begin{cases} -1 & \text{for } \theta < \pi - \nu\pi \\ 0 & \text{for } \pi - \nu\pi \le \theta \le \pi + \nu\pi \\ 1 & \text{for } \theta > \pi + \nu\pi \end{cases}. \tag{7}$$

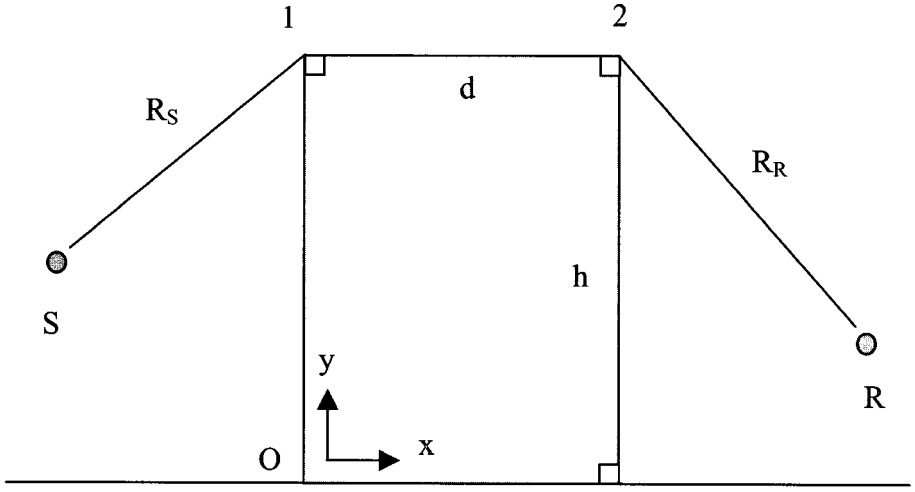

Figure 3. Double diffraction by a wide barrier.

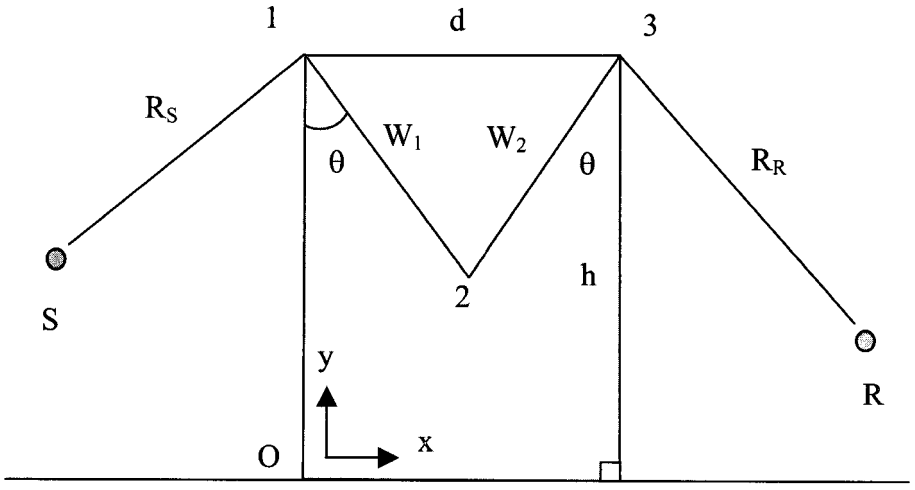

Figure 4. Double (S-1-3-R) or triple diffraction (S-1-2-3-R) by two wedges.

After substituting Eq. (2) into Eq. (1), we rewrite Eq. (1) as

$$\phi = \frac{e^{-ikL}}{L} H_Q \,, \tag{8}$$

where $L = R_S + R_R$, and

$$H_Q = \frac{1}{\sqrt{AB}} D_Q \,. \tag{9}$$

According to Kawai[6], the error associated with Eq. (9) is within 0.5 dB when $R_S,\ R_R \geq \lambda / 4$, in which λ is wavelength.

For double wedges that are separated as shown in Fig. 2, the diffracted wave at receiver point R can be expressed by assuming the wave at point 2 as a source

$$\phi(R) = \phi_i(Q_2) D_2 \sqrt{\frac{R_S + W}{R_R L}}\, e^{-ikR_R} \,, \tag{10}$$

where $\phi_i(Q_2)$ is given in Eq. (8), and $L = R_S + W + R_R$. Note that the distance from the source is taken as $R_S + W$, not W. After substitution of Eqs. (8) and (9) into (10), and rearrangement, we have

$$\phi = \frac{e^{-ikL}}{L} H_1 H_2 \,, \tag{11}$$

where

$$H_1 = \frac{1}{\sqrt{A_1 B_1}} \left[V_1(A_1, B_1, \theta_1 - \theta_{S1}) + V_1(A_1, B_1, \theta_1 + \theta_{S1}) \right], \tag{12}$$

$$H_2 = \frac{1}{\sqrt{A_2 B_2}} \left[V_2(A_2, B_2, \theta_2 - \theta_{S2}) + V_2(A_2, B_2, \theta_2 + \theta_{S2}) \right], \tag{13}$$

in which $A_1 = \left(W + R_R\right) R_S / L$, $A_2 = \left(W + R_S\right) R_R / L$, $B_1 = \rho$, $B_2 = 1$, and

$$\rho = \frac{WL}{(W + R_S)(W + R_R)} \,. \tag{14}$$

Note that changing the source and receiver points in Fig. 2 leads to different expressions from Eqs. (11) – (13). To

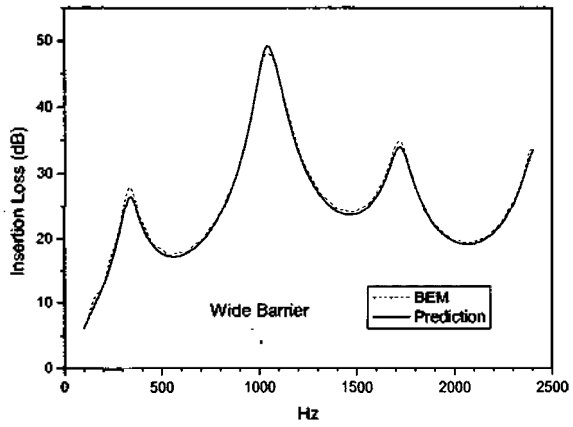

Figure 5. Comparison of insertion loss of a 2D wide barrier by prediction (17) and BEM.

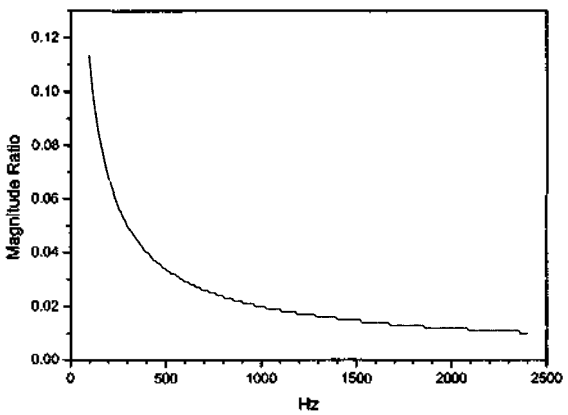

Figure 6. Magnitude ratio of triple (path: S-1-2-3-R) to double diffraction (path: S-1-3-R), $\left|\phi_{triple} / \phi_{double}\right|$ in Fig. 4.

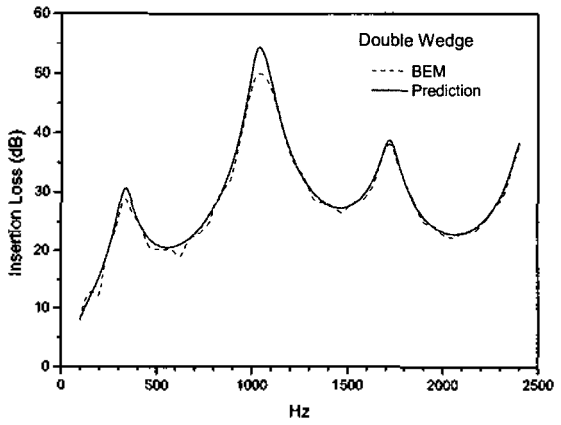

Figure 7. Comparison of insertion loss of double wedges by prediction (11) and BEM

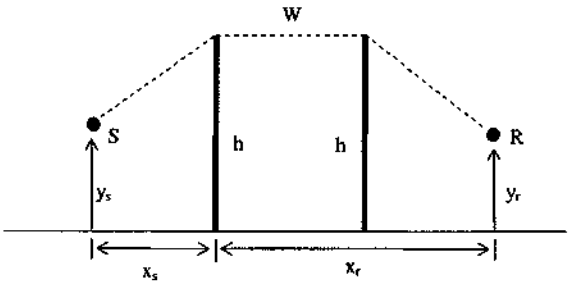

Figure 8. Double knife-edge barrier with W = 1.89 m, x_s = 5 m, y_s = 1.5 m, x_r = 7 m, y_r = 2 m, and h = 3.17 m (taken from Fig. 8 in Ref. [9]).

ensure the continuity of the sound field and reciprocity, we choose the coefficients B_1, B_2 as discussed in Ref. [6] as

$$\text{for}, \quad B_1 = \rho, \; B_2 = 1, \tag{15}$$

$$\text{for } X_1^-(\theta_1 - \theta_{S1}) > X_2^-(\theta_2 - \theta_{S2}), \quad B_1 = 1, \; B_2 = \rho. \tag{16}$$

For the case of a wide barrier in Fig. 3, where two edges are connected, we need to multiply 1/2 to Eq. (11), since there exists a mirror image on the connecting surface

$$\phi = \frac{1}{2}\frac{e^{-ikL}}{L} H_1 H_2. \tag{17}$$

Eqs. (11) and (17) can be extended to more general configuration. If the number of edges is N and number of pairs of neighboring edges that are connected is M respectively, the total diffraction field is given by

$$\phi = \left(\frac{1}{2}\right)^M \frac{e^{-ikL}}{L} \prod_{Q=1}^{N} H_Q, \tag{18}$$

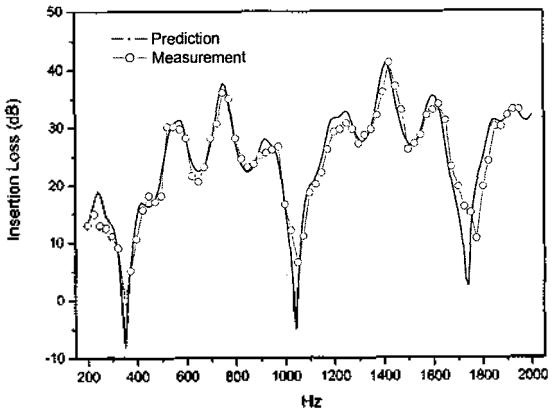

Figure 9. Insertion loss of double knife-edge barrier in Fig. 8. Measurement data is from Ref. [9].

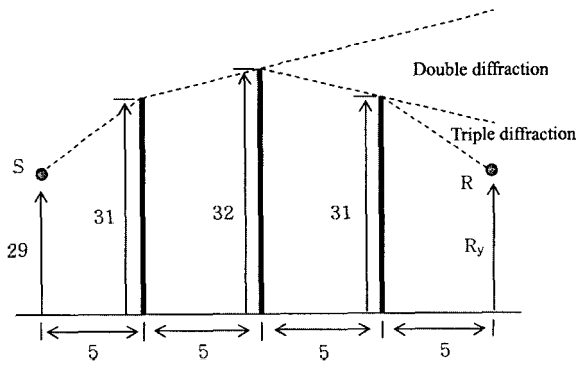

Figure 10. Triple barriers (taken from Fig. 1 in Ref. [11]). All units are in meter.

where L is the traveled distance. It is worth noting that Eq. (18) can be applied to the case that there exist convex and concave edges simultaneously. For instance, diffraction for the path S-1-2-3-R in Fig. 4 is given by

$$\phi = \left(\frac{1}{2}\right)^2 \frac{e^{-ikL}}{L} H_1 H_2 H_3, \tag{19}$$

in which, $L = R_S + W_1 + W_2 + R_R$, whereas diffraction for the path S-1-3-R is given by Eq. (11) with $L = R_S + d + R_R$.

In case of two-dimensional wave, we need to replace e^{-ikL}/L in Eqs. (8), (11), (17) and (18) by $(-i/4)H^{(2)}(kL)$ (more strictly, asymptotic form of Hankel function when $kL >> 1$).

III. Numerical examples

As the first numerical example, we consider a two-dimensional wide barrier in Fig. 3 where S=(-13,0.5), R=(5, 0.5), $d = 1.5$, $h = 2$, in which all units are in meter. Here,

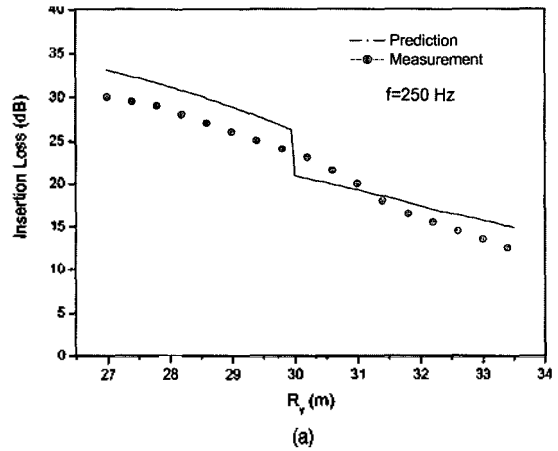

(a)

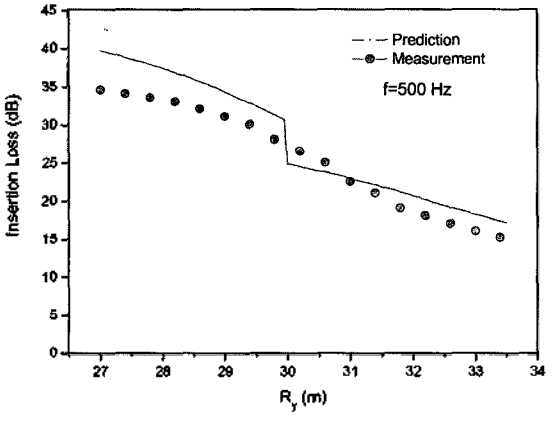

(b)

Figure 11. Comparisons of insertion loss for triple barriers in Fig. 10. (Measurement data are from Ref. [11].)

we take into account the reflection from the ground. For comparison, we performed numerical analysis by using the BEM and compared the numerical results to theoretical prediction by using Eq. (17) in Fig. 5. In BEM, we model the upper half plane ($y \geq 0$), for which we modify the Green function to take into account the reflection from rigid ground

$$G(\mathbf{r}, \mathbf{r}') = (-i/4)[H^{(2)}(k\,|\,\mathbf{r}-\mathbf{r}'\,|) + H^{(2)}(k\,|\,\mathbf{r}_m-\mathbf{r}'\,|)], \quad (20)$$

in which vector $\mathbf{r}$ refers to the point to be computed, $\mathbf{r}_m$ is the image point of $\mathbf{r}$ with respect to the ground, and $\mathbf{r}'$ refers to the point on the integration domain. The modified Green function makes the normal derivative vanish on the ground

$$\partial G / \partial n(\mathbf{r}') = 0 . \quad (21)$$

We employed three-noded quadratic element, where there is about 10 elements within one wavelength at 2.5 kHz. The insertion loss is defined as

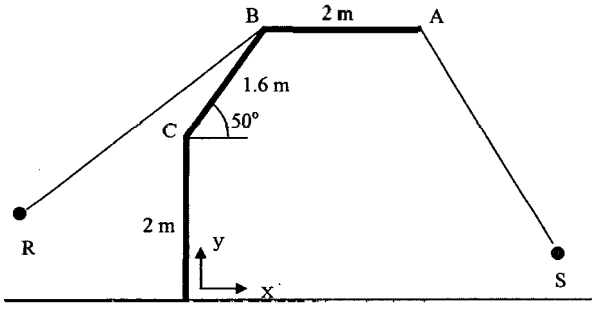

Figure 12. Doubly inclined barrier.

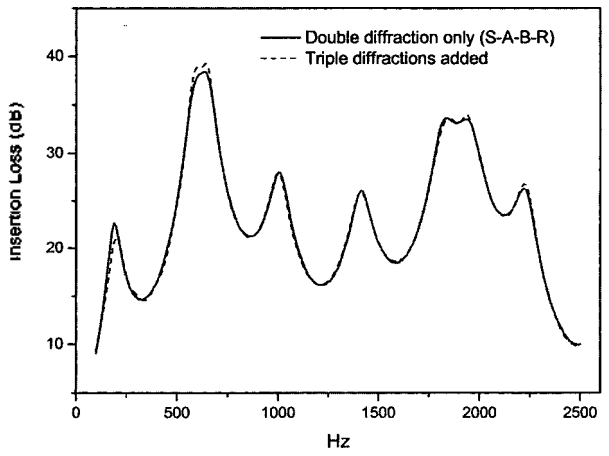

Figure 13. Insertion loss of the doubly inclined barrier in Fig. 12 when S = (15 m, 0.5 m), and R = (-10 m, 1.5 m).

$$IL = 20\log\left|\phi_0 / \phi_{barrier}\right| , \quad (22)$$

where ϕ_0 is the sound field without barrier

$$\phi_0 = \sum_j \exp(-ikL_j)/L_j , \quad (23)$$

in which $i (i = 1, 2)$ denotes two paths with and without ground reflections. Fig. 5 shows that theoretical prediction of insertion loss agrees well with the BEM result.

The next example is double wedges in Fig. 4, where all configurations are the same as in Fig. 3 except that convex edge is added at the center to form two wedges with $\theta = 36.9^{\circ}$, $W_1 = W_2 = 1.25$ m. We compared magnitude ratio of triple diffraction (path: S-1-2-3-R) to double diffraction (path: S-1-3-R), $\left|\phi_{triple} / \phi_{double}\right|$ in Fig. 6, which shows that the ratio is less than 0.04 except low frequency (f < 400 Hz). In Fig. 7, we compared theoretical prediction including only double diffraction to BEM result, which shows good agreement except peak around 1 kHz.

For double barriers on the rigid ground as shown in Fig. 8, Wadsworth and Chambers[9] performed 1/10 scale model experiment. They used electric sparks as the sound source, which generates a transient pulse of duration 100μs. They transformed time domain data into frequency-based insertion loss after FFT process. In this paper, we computed insertion loss by using Eq. (11) and compared the results in Fig. 9, which shows excellent agreement.

For triple barriers shown in Fig. 10, Higashi *et al.*[11] measured insertion loss by using 1/40 scale model, while varying height of microphone, R_y . Depending on the height of receiver position, wave propagation may change from triple diffraction to direct path. Here, we computed insertion loss for double ($30 < R_y < 34$) and triple diffraction ($R_y < 30$) . We compared the predictions with measurements in Fig. 11(a) and 11(b) for 250 Hz and 500 Hz, where no ground reflections are included. Figs. 11 show that two results differ by 2-4dB, which may be due to reflections from the ground. Note that predictions show abrupt changes across $R_y = 30$, whereas measurements vary smoothly.

For the final example, we consider a doubly inclined barrier in Fig. 12. The source and receiver positions are: S=(15 m, 0.5 m); R=(-10 m, 1.5 m). We compared two cases: only double diffraction, ϕ_{SABR} and double and triple

diffractions, $\phi_{SABR} + \phi_{SABCR} + \phi_{SBABR}$. Fig. 13. shows that insertion loss may be represented by only double diffraction with sufficient accuracy.

IV. Concluding remarks

We have presented a GTD-based formula that can compute sound diffraction by multiple wedges, barriers, or polygonal-like shapes. Both convex and concave edges can be allowed in the formula, while edges may or may not be inter-connected. Comparisons of theoretical predictions with other results done by the BEM or experiments for scaled model have confirmed the accuracy of the present formula. Numerical examples such as double wedges and doubly inclined barrier have revealed that when there exist several diffraction paths for given source and receiver positions, the insertion loss is dominated by the diffraction associated with the shortest path.

References

1. D. Ouis, "Noise attenuation by a hard wedge-shaped barrier", Journal of Sound and Vibration, **262**, 347-364, 2003.
2. R. G. Kouyoumjian and P. H. Pathak, "A uniform geometrical theory of diffraction for an edge in a perfectly conducting surface", Proceedings of the IEEE, **62**, 1448-1461, 1974.
3. A. D. Pierce, "Diffraction of sound around corners and over wide barriers", Journal of the Acoustical Society of America, **55**, 941-955, 1974
4. W. T. Hadden and A. D. Pierce, "Sound diffraction around screens and wedges for arbitrary point source locations", Journal of the Acoustical Society of America, **69**, 1266-1276, 1981, Erratum, 71, 1290, 1982.
5. E. M. Salomons, "Sound propagation in complex outdoor situations with a non-refracting atmosphere: model based on analytical solutions for diffraction and reflection", Acustica, **83**, 436-454, 1997.
6. T. Kawai, "Sound diffraction by a many-sided barrier or pillar", Journal of Sound and Vibration, **79**, 229-242, 1980.
7. Byung-Joo Jin, Hyun-Sil Kim, Hyun-Ju Kang, and Jae-Seung Kim, "Sound diffraction by a partially inclined noise barrier", Applied Acoustics, **62**, 1107-1121, 2000.
8. J. S. Robertson, "Sound propagation over a large wedge: a comparison between the geometrical theory of diffraction and the parabolic equation", Journal of the Acoustical Society of America, **106**, 113-119, 1999.
9. G. J. Wadsworth and J. P. Chambers, "Scale model experiments on the insertion loss of wide and double barriers", Journal of the Acoustical Society of America, **107**, 2344-2350, 2000.
10. M. A. Biot and I. Tolstoy, "Formulation of wave propagation in infinite media by normal coordinates with an application to diffraction", Journal of the Acoustical Society of America, 29, 381-391, 1957.
11. K. Higashi, Y. M. Park, K. Takagi, R. Hotta, and K. Yamamoto, "Noise attenuation by triple barriers", Proceeding of Technical Presentation of Noise Control in Japan (in Japanese), 297-300, 1995.

[Profile]

● Hyun-Sil Kim
The Journal of the Acoustical Society of Korea, Vol. 21, No.1E, 2002

● Jae-Sueng Kim
The Journal of the Acoustical Society of Korea, Vol. 21, No.1E, 2002

● Hyun-Ju Kang
The Journal of the Acoustical Society of Korea, Vol. 21, No.1E, 2002

● Bong-Kim
The Journal of the Acoustical Society of Korea, Vol. 21, No.1E, 2002

● Sang-Ryul Kim
The Journal of the Acoustical Society of Korea, Vol. 21, No.1E, 2002